The role of the innate and adaptive immune system on vascular remodeling

Simons, K.H.

Chapter 7

A protective role of IRF3 and IRF7 signaling downstream TLRs in the development of vein graft disease via type-I interferons.

K.H. Simons, H.A.B. Peters, J.W. Jukema, M.R. de Vries, P.H.A. Quax.

Journal of internal medicine. 2017;282(6):522-536.

Abstract

Background

Toll like receptors (TLR) play an important role in vein graft disease (VGD). Interferon regulatory factors (IRF) 3 and 7 are the transcriptional regulators of type-I interferons (IFN) and type-I IFN responsive genes and are downstream factors of TLRs. Relatively little is known with regard to the interplay of IRFs and TLRs in VGD development. The aim of this study was to investigate the role of IRF3 and IRF7 signaling downstream TLRs and the effect of IRF3 and IRF7 in VGD.

Methods and Results

In vitro activation of TLR3 induced IRF3 and IRF7 dependent IFNβ expression in bone marrow macrophages and vascular smooth muscle cells. Activation of TLR4 showed to regulate pro-inflammatory cytokines via IRF3. Vein graft surgery was performed in *Irf3*$^{-/-}$, *Irf7*$^{-/-}$ and control mice. After 14 days *Irf3*$^{-/-}$ vein grafts had an increased vessel wall thickness compared to both control (p=0.01) and *Irf7*$^{-/-}$ (p=0.02) vein grafts. After 28 days, vessel wall thickness increased in *Irf3*$^{-/-}$ (p=0.0003) and *Irf7*$^{-/-}$ (p=0.04) compared to control vein grafts and also increased in *Irf7*$^{-/-}$ compared to *Irf3*$^{-/-}$ vein grafts (p=0.02). Immunohistochemical analysis showed a significant higher influx of macrophages after 14 days in *Irf3*$^{-/-}$ vein grafts and after 28 days in *Irf7*$^{-/-}$ vein grafts compared to control vein grafts.

Conclusions

The present study is the first to describe a protective role of both IRF3 and IRF7 in VGD. IRFs regulate VGD downstream TLRs since *Irf3*$^{-/-}$ and *Irf7*$^{-/-}$ vein grafts show increased vessel wall thickening after respectively 14 and 28 days after surgery.

Introduction

Arterial occlusive disease is an atherosclerosis driven chronic disease that causes impaired blood flow. In case of severe arterial occlusive disease, bypass surgery is performed with the vena saphena magna as the most used conduit. Unfortunately, long term graft patency rates are low due to vein graft disease (VGD)[1, 2]. Development of intimal hyperplasia (IH) in vein grafts consist of several phases, the first days an influx of inflammatory cells such as macrophages occurs, followed by extracellular matrix breakdown and subsequent remodeling as well as proliferation and migration of vascular smooth muscle cells (VSMCs).

We and others have shown that Toll-like receptors (TLRs), important members of the innate immune system, are involved in intimal hyperplasia formation, accelerated atherosclerosis and vein graft remodeling[3-5] via recognition of pathogen-associated molecular patterns and damage associated molecular patterns[6]. Interestingly, a protective role of TLR3 was found on the onset of atherosclerosis formation[7]. TLR3 stimulation also impaired endothelial function[8] and deficiency of TLR3 resulted in increased atherosclerotic lesion burden[9]. TLRs, except TLR3, signal via myeloid differentiation primary response gene 88 (MyD88) pathway, which drives the induction of the transcription factor nuclear factor kappa-light-chain-enhancer of activated B cells (NF-κB) resulting in pro-inflammatory cytokines production[10]. TLR3, and sometimes TLR4, signals via a MyD88-independent pathway which induces type-I IFN production, and sometimes pro-inflammatory cytokine production, via TIR-domain-containing adaptor protein inducing IFNβ (TRIF) in various cell types[11].

Interferon regulatory factor (IRF) 3 and 7 are downstream factors of TLRs and play important roles in innate immunity through the transcriptional regulation of type-I IFNs such as IFNα and IFNβ. IFNα and IFNβ have shown to play a role in cardiovascular diseases with analogous pathophysiology as vein graft disease [12]. IRF3 is a potent activator of the IFNβ gene but not the IFNα genes, except the IFNα4 gene, whereas IRF7 efficiently activates both IFNα and IFNβ genes[4, 13]. IRF3 is primarily responsible for the induction of t*ype-I IFN* genes in the early induction phase[14]**.** IRF3 resides in the cytosol in a latent form and after activation by phosphorylation, IRF3 causes IFNβ synthesis and signal transduction through the type-I IFN receptor IFNAR[4, 15]. IRF7 also resides in the cytosol, but is expressed in a low amount. However, IFNAR signal transduction increases IRF7 protein expression[16] and IRF7 then causes a late induction of both IFNα and IFNβ, where it induces a positive-feedback loop via repeated IFNAR binding[17-19]. Blocking the IFNAR resulted in the induction of vascular remodeling in a mouse model for hind limb ischemia[12].

Recent studies have shown that IRFs play critical roles in diseases with (partial) analogous pathophysiology as vein graft disease such as antiviral defence[17], cardiac remodeling[20], multiple sclerosis[21] and inflammasome activation[22], indicating that there might also be a role for IRFs in VGD. However, the signaling pathways downstream TLR3 and TLR4 in VSMCs and bone marrow macrophages (BMM) are not yet completely clarified and the exact role of IRF3 and IRF7 signaling downstream TLRs and type-I IFNs in VGD is unclear.

In the current study, we investigate the role of IRF3 and IRF7 signaling downstream TLRs *in vitro* by using VSMCs and BMM and the role of IRF3 and IRF7 *in vivo* in vein graft disease in a murine vein graft model, using wild type, *Irf3*$^{-/-}$ and *Irf7*$^{-/-}$ mice.

Material and methods

Mice

This study was performed in compliance with Dutch government guidelines and the Directive 2010/63/EU of the European Parliament. All animal experiments were approved by the animal welfare committee of the Leiden University Medical Center. For the experiments 10 to 18 week old male mice were used. We performed multiple *in vitro* and *in vivo* studies in wild type C57BL/6 mice purchased from Charles River Laboratories and *Irf3*$^{-/-}$ and *Irf7*$^{-/-}$ mice that were kindly provided by Dr. Taniguchi (University of Tokyo, Japan) and bred in our facility. Mice were fed a chow diet ad libitum.

Vein graft surgery

Vein graft surgery was performed by donor caval vein interpositioning in the carotid artery of recipient mice[23]. At day of the surgery caval veins were harvested (t=0). After 7 days (t=7), 14 days (t=14) and 28 days (t=28) mice were sacrificed and vein grafts were harvested. Both before surgery and sacrifice, mice were anesthetized with a combination of intraperitoneal injected Midazolam (5 mg/kg, Roche), Medetomidine (0.5 mg/kg, Orion) and Fentanyl (0.05 mg/kg, Janssen). Buprenorphine (0.1 mg/kg, MSD Animal Health) was given after surgery to relieve pain in a fixed regime and when circumstances required this was repeated.

Histological and immunohistochemical assessment of vein grafts

Vein graft samples were embedded in paraffin and sequential cross sections (5 µm thick) were made throughout the embedded vein grafts. To quantify the vein graft thickening (vessel wall area), HPS staining was performed using Hematoxylin, Phloxin 0.25%, and

Saffron 0.3%. Total size of the vein graft (total vessel area) and lumen was measured. Thickening of the vessel wall (vessel wall thickening) was defined as the area between lumen and adventitia and determined by subtracting the luminal area from the total vessel area. Antibodies directed at alpha smooth muscle cell actin (aSMActin, Sigma), IRF3, IRF7 (Abcam) and Mac-3 (BD Pharmingen) were used for immunohistochemical staining**.** Sirius red staining (Klinipath 80115) was performed to quantify the amount of collagen present in the vein grafts. The immuno-positive area measured is expressed as a percentage of the vessel wall area. Stained slides were photographed using microscope photography software (Axiovision, Zeiss) and image analysis software was used to quantify the vein graft intimal hyperplasia and composition (Qwin, Leica).

Proliferation analysis

Immunohistochemical staining was performed for proliferation marker Ki67, combined with aSMActin, on vein grafts of *Irf3*$^{-/-}$**,** *Irf7*$^{-/-}$ and control mice sacrificed at 28 days. The number of proliferating cells (Ki67 positive cells) and the number of proliferating smooth muscle cells (Ki67 and aSMActin positive cells) was quantified by manual counting of the number of cells per high power magnification and expressed as percentage of total cells.

Cell culture

BMM were acquired by isolating monocytes from femur and tibia bone marrow of *Irf3*$^{-/-}$, *Irf7*$^{-/-}$ and control mice. 5 x 10^5 Cells were cultured per well of 6-wells FALCON® plates, with 3 wells per group (BD Biosciences) with RPMI 1640 medium supplemented with 25% heat-inactivated FCS (Gibco® by Life Technologies) and 100 U/mL Penicillin/streptomycin (Gibco® by Life Technologies) in the presence of 0.1mg/ml macrophage colony-stimulating factor (M-CSF). After seven days, the BMM were seeded and after 24 hours, when macrophages were fully attached, they were stimulated with established exogenous ligands for TLR3 and TLR4: 100 µg/ml Polyinosinic-polycytidylic acid (PolyI:C) purchased from InvivoGen (CA) and 100ng/ml Lipopolysaccharide from Escherichia coli K-235 (LPS) purchased from Sigma-Aldrich (MO, USA) respectively. After 1, 3, 7 and 24 hour supernatant was collected for ELISA and RNA was isolated from stimulated cells using TRIzol® (Ambion® by Life Technologies).

Irf3$^{-/-}$, *Irf7*$^{-/-}$ and control VSMCs were acquired by isolating VSMCs from mice aortas. Cells were cultured in medium containing DMEM Glutamax with 20% FCS, non-essential amino acids (MEM 100x, Gibco® by Thermo Fisher) and 100 U/mL Penicillin/streptomycin. Cells were passaged when a confluence of 90-95% was reached. 10^5 VSMCs were plated in a 48 wells plate, and stimulated with culture medium. After 24 hours, cells were stimulated with 100 µg/ml PolyI:C and 100ng/ml LPS respectively.

After 1, 3, 7 and 24 hour, supernatant was collected for ELISA and RNA was isolated from stimulated cells using TRIzol®.

Detection of protein levels of IFNβ, CCL2 and TNFa.

IFNβ production was measured after 1, 3, 7 and 24 hour in supernatant of VSMCs and BMM using a LEGEND MAX™ mouse IFNβ ELISA kit with pre-coated plates (BioLegend) according to manufacturer's protocol. Pro-inflammatory cytokines CCL2 and TNFα was measured using a BD OptEIA™ mouse ELISA kit (BD Biosciences) in supernatant of VSMC and BMM, according to manufacturer's protocol.

RNA isolation, cDNA synthesis and RT-qPCR from cell cultures

RNA was isolated from BMM and VSMCs after 1, 3, 7 and 24 hour of PolyI:C or LPS stimulation and was quantified using a NanoDrop 1000 Spectrophotometer (Thermo Scientific). cDNA was synthesized using a High-Capacity cDNA Reverse Transcription Kit (Applied Biosystems). To measure the expression of the type-I IFN inducible genes, *Ifit (*Assay ID, Mm00515153_m1, Thermo Fisher) and *Mx1* ((Assay ID, Mm00487796_m1, Thermo Fisher), RT-qPCR was performed using TaqMan (Thermo Fisher). To measure the expression of type-I IFN, IFNβ (forward GGAGATGACGGAGAAGATGC, reverse CCCAGTGCTGGAGAAATTGT), RT-qPCR was performed using QuantiTect SYBR Green PCR Kit (Qiagen). GAPDH (Applied Biosystems) was used as a housekeeping gene. All RT-qPCRs were performed on a 7500/7500 Fast Real-Time PCR System (Applied Biosystems) and the 2-ΔΔCt method was used to analyse the relative changes in gene expression.

RNA isolation, cDNA synthesis and RT-PCR from vein graft tissue

Total RNA was isolated from 10 (20µm thick) paraffin sections of vein grafts 28d after surgery (n=6/strain). RNA was isolated according manufacturers protocol (FFPE RNA isolation kit, Qiagen). FFPE RNA was reverse transcribed using the RT^2 First Strand Kit (SA Biosciences). RNA for single Q-PCR was reverse transcribed using a High-Capacity cDNA Reverse Transcription Kit (Applied Biosystems) according to the manufacturer's protocol. Commercially available TaqMan gene expression assays for hypoxanthine phosphoribosyltransferase (HPRT1), and selected genes of interest were used (Applied Biosystems). qPCR analysis of 84 type-I IFN responsive genes was performed using a RT^2 Profiler PCR Array (SA Biosciences) according to the manufacturer's protocol. The complete list of the genes analysed is available at http://www.sabiosciences.com/rt_pcr_product/HTML/PAMM-016Z.html. Prior to RT^2 profiler array, all qPCRs were performed on a 7500/7500 Fast Real-Time PCR System and the 2-ΔΔCt method was used to analyse the relative changes in gene expression.

Statistical analysis

All data are presented as mean ± SEM. In statistics software GraphPad Prism 7.0, statistical analyses on parametric data were performed by using a 2-tailed Student's t-test to compare individual groups, Mann-Whitney test was used for nonparametric data. A 1-way ANOVA was performed on parametric data comparing more than 2 groups and a Kruskal-Wallis test was performed on nonparametric data. P value of <0.05 was considered significant.

Results

Type-I IFN production in VSMCs is exclusively regulated downstream TLR3 and pro-inflammatory cytokine production downstream TLR3 and TLR4.

To investigate whether the production of the type-I IFN IFNβ and pro-inflammatory cytokine production of CCL2 is regulated downstream TLR3 or TLR4 pathways in VSMCs, we stimulated VSMC with TLR3 ligand PolyI:C , TLR4 ligand LPS or PBS as control. After 6 hours and 8 hours IFNβ production of VSMCs stimulated with PolyI:C showed a respectively 3.2 fold increase (p=0.04) and 3.7 fold increase (p=0.02) compared to control (figure 1a). LPS and control showed no increase in IFNβ production over time, indicating that IFNβ production is specific downstream TLR3 in VSMCs.

CCL2 production of LPS stimulated VSMC showed a significant 10.2 fold increase (p=0.003) after 6 hours and also after 8 hours with an 18.4 fold increase (p<0.0001) compared to control (figure 1b). In PolyI:C stimulated VSMCs an 8.7 fold increase after 6 hours was observed (p=0.001) and a 9.6 fold increase after 8 hours (p=0.003) compared to control, indicating a regulation of pro-inflammatory cytokine production downstream TLR3 and TLR4 in VSMCs.

IRF3 and IRF7 signal downstream TLR3 and IRF3 downstream TLR4 in BMM.

To determine the role of IRF3 and IRF7 in the downstream signaling pathways of TLR3 and TLR4, type-I IFN inducible genes, *Ifit* and *Mx1*, were measured in *Irf3*$^{-/-}$, *Irf7*$^{-/-}$ and control BMM. In *Irf3*$^{-/-}$ BMMs stimulated with PolyI:C the mRNA expression of *Ifit* was significantly reduced by 75% compared to the control group whereas the mRNA expression of *Mx1* was significantly reduced by 80%. Also in *Irf7*$^{-/-}$ BMMs stimulated with PolyI:C the mRNA expression of *Ifit* was significantly reduced by 79% and the mRNA expression of *Mx1* was significantly reduced by 96% compared to the control group (figure 2a), indicating a strong signaling pathway of IRF3 and IRF7 downstream TLR3 in BMM. Interestingly, *Mx1* mRNA expression showed a 81% reduction in *Irf7*$^{-/-}$ BMM

compared to *Irf3*$^{-/-}$ BMM (p=0.0005), suggesting a stronger effect of IRF7 on type-I IFN transcription then IRF3 downstream TLR3 in BMM.

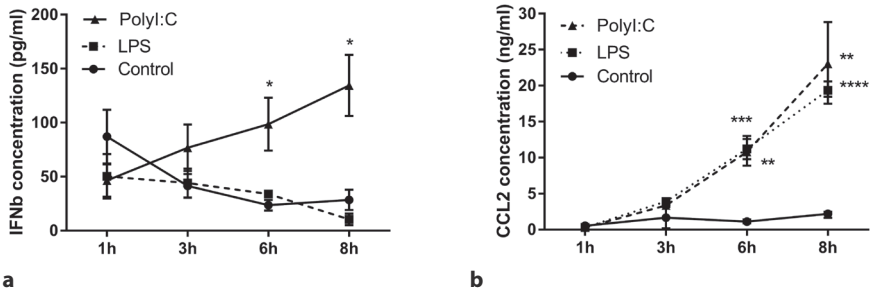

Figure 1. Stimulation of control VSMCs with either PolyI:C, LPS or control medium. After 1, 3, 6 and 8 hour supernatant was collected and cytokine production was measured with ELISA. **a.** IFNβ concentration (pg/ml) is shown **b.** CCL2 concentration (ng/ml) is shown. Results are depicted as mean ± SEM *p<0.05, **p<0.01, *** p<0.001. **** p<0.0001. n=3

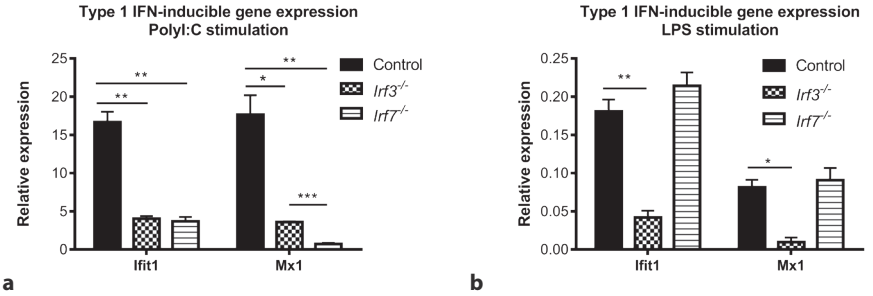

Figure 2 BMM of *Irf3*$^{-/-}$, *Irf7*$^{-/-}$ and control mice were stimulated for 24h after which RNA was harvested for RT-qPCR analysis **a.** stimulation with 30 µg/ml PolyI:C **b.** stimulation with 100 ng/ml LPS. Results are depicted as mean ± SD versus control. *p<0.05, **p<0.01, *** p<0.001. n=3

We evaluated whether IRF3 and IRF7 were also involved in downstream TLR4 signaling pathway, by stimulation of BMM with LPS. *Irf3*$^{-/-}$ BMM showed a significant down regulation of 77% of *Ifit1* and 88% of *Mx1* mRNA expression compared to the controls (Figure 2b). Moreover, the type-I IFN inducible gene mRNA expression levels were not affected in BMM of *Irf7*$^{-/-}$ mice, indicating that IRF7 signaling is not regulated downstream TLR4, whereas IRF3 signaling is more specifically regulated downstream TLR4 in BMM.

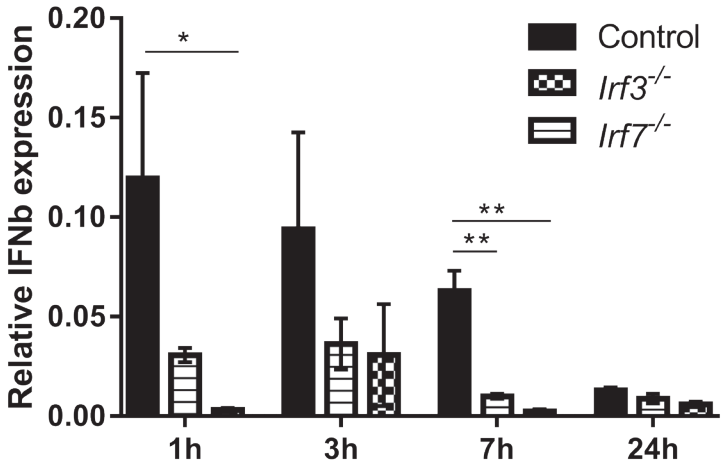

Figure 3. *Irf3*$^{-/-}$, *Irf7*$^{-/-}$ and control BMM were stimulated with 100 µg/ml PolyI:C for 1, 3, 7 and 24 hour after which RNA was harvested for RT-qPCR analysis. Relative IFNβ mRNA expression to GAPHD is shown. *p<0.05, **p<0.01, *Irf3*$^{-/-}$ n=3, *Irf7*$^{-/-}$ n=9, control n=12

Type-I IFN transcription downstream TLR3 is IRF3 and IRF7 dependent in BMM.

To determine whether IRF3 and IRF7 are involved in the transcription of the type-I IFN IFNβ downstream TLR3, we stimulated BMM of *Irf3*$^{-/-}$, *Irf7*$^{-/-}$ and control mice with PolyI:C and measured IFNβ mRNA expression. In *Irf3*$^{-/-}$ BMM IFNβ mRNA expression was decreased after 1 hour (p=0.02) compared to control (figure 3). Both *Irf3*$^{-/-}$ (p=0.001) and *Irf7*$^{-/-}$ (p=0.009) BMM expressed significantly lower IFNβ mRNA levels compared to control after 7 hours of stimulation. Moreover, IFNβ mRNA levels after 1 hour and 7 hours showed a trend towards a decrease in *Irf3*$^{-/-}$ compared to *Irf7*$^{-/-}$ BMM. In conclusion, IRF3 and IRF7 were shown to be responsible for IFNβ transcription in BMM, were IRF3 showed to regulate early IFNβ mRNA expression levels and IRF7 showed to be a late regulator.

IRF3 but not IRF7 is involved in pro-inflammatory cytokine production in BMM.

We have shown that pro-inflammatory cytokine production can be induced via TLR3 and TLR4 signaling (figure 1) and that type-I IFNs can be regulated via IRF3 and IRF7downstream TLR3 and downstream TLR4 via IRF3 (figure 2). To determine the role of IRF3 and IRF7 in pro-inflammatory cytokine production, we measured CCL2 and

TNFα production of PolyI:C stimulated BMM of *Irf3*$^{-/-}$, *Irf7*$^{-/-}$ and control mice. *Irf3*$^{-/-}$ BMM showed a significant reduction in CCL2 production after 7 hours compared to both control (p=0.02) and *Irf7*$^{-/-}$ BMM (p=0.007) (figure 4a). Moreover, TNFα production of *Irf3*$^{-/-}$ BMM was significantly decreased compared to control after 3 hours (p=0.004) and 7 hours compared to both control (p<0.0001) and *Irf7*$^{-/-}$ BMM (p=0.003) (figure 4b). *Irf7*$^{-/-}$ BMM showed no differences in both CCL2 and TNFα production compared to control. In conclusion, we here show an IRF3 dependent, and not IRF7 dependent, regulation of *in vitro* pro-inflammatory cytokine production in BMM.

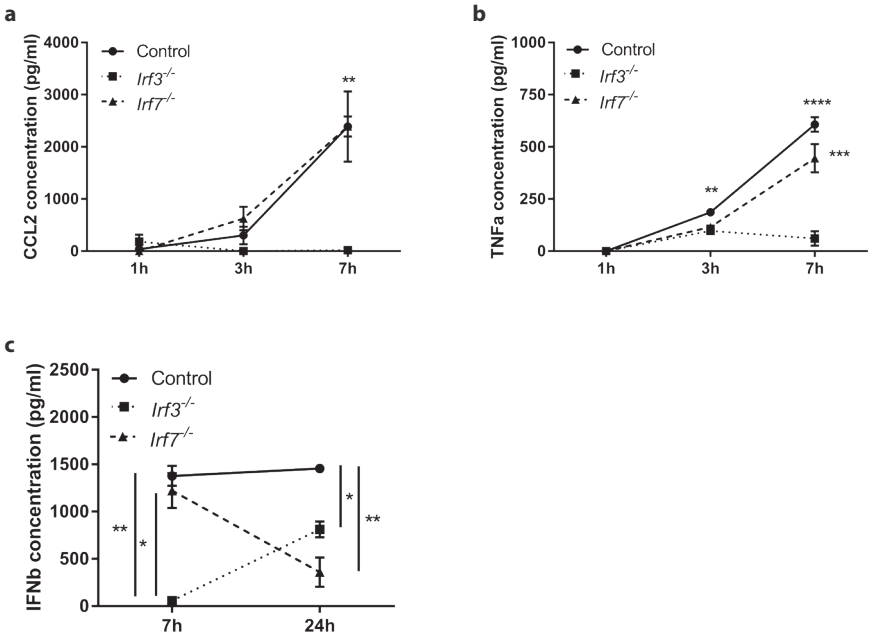

Figure 4 *Irf3*$^{-/-}$, *Irf7*$^{-/-}$ and control BMM were stimulated with 100µg/ml PolyI:C . **a**. After 1, 3 and 7 hour supernatant was collected and cytokine production of CCL2 (pg/ml) and **b.** TNFα (ng/ml) was measured with ELISA. t=1h and t=7h; n=8, t=3h; n=4. **c.** IFNβ production (pg/ml) was measured after 7 and 24 hours. n=4 Results are depicted as mean ± SEM. *p<0.05, **p<0.01, **** p<0.0001.

Type-I IFN production downstream TLR3 is IRF3 and IRF7 dependent.

To determine the role of IRF3 and IRF7 in the production of the type-I IFN IFNβ downstream TLR3, we stimulated BMM of *Irf3*$^{-/-}$, *Irf7*$^{-/-}$ and control mice with PolyI:C and measured IFNβ production. In *Irf3*$^{-/-}$ BMM a decreased IFNβ production was measured after 7 hours in compared to both control (p=0.004) and *Irf7*$^{-/-}$ BMM (p=0.002) (figure 4c). Interestingly, after 24 hours of PolyI:C stimulation *Irf3*$^{-/-}$ and *Irf7*$^{-/-}$ BMM showed

opposite results with lower IFNβ production of *Irf7*$^{-/-}$ BMM compared to *Irf3*$^{-/-}$ BMM (p=0.05). After 24 hours, both *Irf7*$^{-/-}$ BMM (p=0.009) and *Irf3*$^{-/-}$ BMM (p=0.007) showed a decreased IFNβ production compared to control. In conclusion, we here show an important role of IRF3 in early type-I IFN production and a role of IRF7 in late type-I IFN production.

IRF3 and IRF7 deficiency causes increased vein graft remodeling in time.

Both IRF3 and IRF7 are expressed in vein grafts of control mice after 28 days. Both cytoplasmic as well as nuclear staining was seen indicating that latent and active forms of IRF3 (figure 5a) and IRF7 (figure 5b) are present. Vein graft showed a more intense nuclear staining of IRF3 and showed both nuclear and cytoplasmic staining of IRF7, indicating not only a constitutive expression of IRF7, but also an induced IRF7 expression in mature vein grafts.

To determine the effect of IRF3 and IRF7 on the total size of the vein graft (total vessel area), thickening of the vessel wall (vessel wall thickening) and lumen area of *Irf3*$^{-/-}$ and *Irf7*$^{-/-}$ vein grafts were compared with control vein grafts. Vessel wall thickening in control, *Irf3*$^{-/-}$ as well as *Irf7*$^{-/-}$ mice increased over time after surgery (figure 5c). At day of the surgery caval veins of *Irf3*$^{-/-}$ mice were significantly 2.1 fold smaller in size (p=0.03) (supplemental figure 1a,c,e,g) and had a significantly 2.6 fold thinner vessel wall (p=0.007) (figure 5d) compared to control caval veins, whereas no differences were observed in lumen size (supplemental figure 1b,d,f,h). No differences were observed between *Irf7*$^{-/-}$ caval veins compared to controls and *Irf3*$^{-/-}$ caval veins (figure 5d and supplemental figure 1). After 7 days, no differences in total vessel area, lumen area (supplemental figure 1) and vessel wall thickening (figure 5d) were observed between *Irf3*$^{-/-}$, *Irf7*$^{-/-}$ and control vein grafts. After 14 days *Irf3*$^{-/-}$ vein grafts had a significantly 1.8 fold increased vessel wall thickening compared to control (p=0.0099) and 1.5 fold increase compared to *Irf7*$^{-/-}$ (p=0.02) vein grafts (figure 5d), but no differences were observed in total vessel area and lumen area (supplemental figure 1b,d,f,h). However, after 28 days vessel wall thickening was significantly 1.7 fold increased in *Irf7*$^{-/-}$ (p=0.0003) and 1.4 fold increased in *Irf3*$^{-/-}$ (p=0.04) vein grafts compared to control vein grafts (figure 5d) and *Irf7*$^{-/-}$ also showed an significantly 1.2 fold increase in vessel wall thickening compared to *Irf3*$^{-/-}$ vein grafts after 28 days (p=0.02). Total vessel wall area was significantly 1.4 fold increased in *Irf7*$^{-/-}$ vein grafts (p=0.04) and lumen area showed no differences (supplemental figure 1).

Here we show an increased vessel wall thickening in vein grafts of *Irf3*$^{-/-}$ and *Irf7*$^{-/-}$ mice, indicating a protective effect of both IRF3 and IRF7 with a stronger protective effect of IRF3 in vein graft disease compared to IRF7 after 14 days, and a stronger protective effect of IRF7 after 28 days.

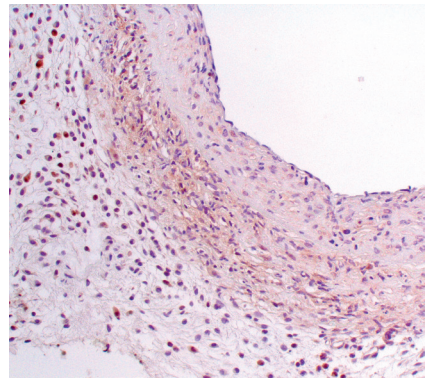

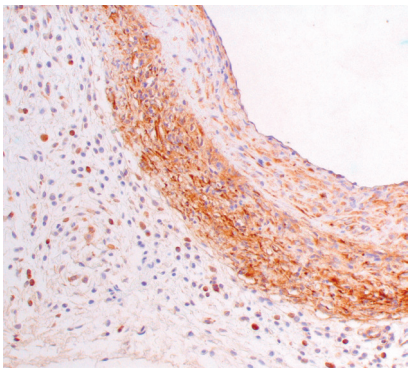

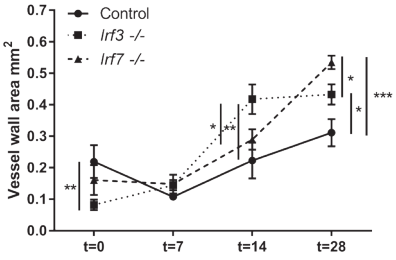
Control
Irf3 -/-
Irf7 -/-
Vessel wall area mm2
0.7
0.6
0.5
0.4
0.3
0.2
0.1
0.0
t=0
t=7
t=14
t=28
**
*
**
*
*
***

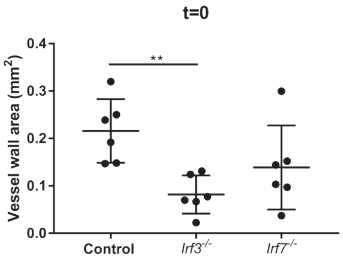
t=0
Vessel wall area (mm2)
0.4
0.3
0.2
0.1
0.0
**
Control
Irf3-/-
Irf7-/-

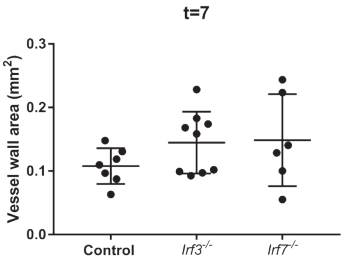
t=7
Vessel wall area (mm2)
0.3
0.2
0.1
0.0
Control
Irf3-/-
Irf7-/-

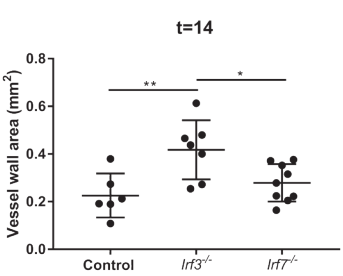
t=14
Vessel wall area (mm2)
0.8
0.6
0.4
0.2
0.0
**
*
Control
Irf3-/-
Irf7-/-

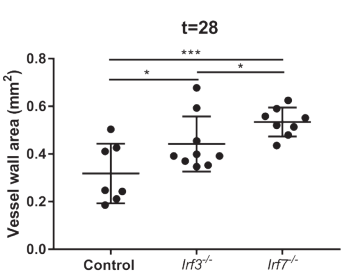
t=28
Vessel wall area (mm2)
0.8
0.6
0.4
0.2
0.0
***
*
*
Control
Irf3-/-
Irf7-/-

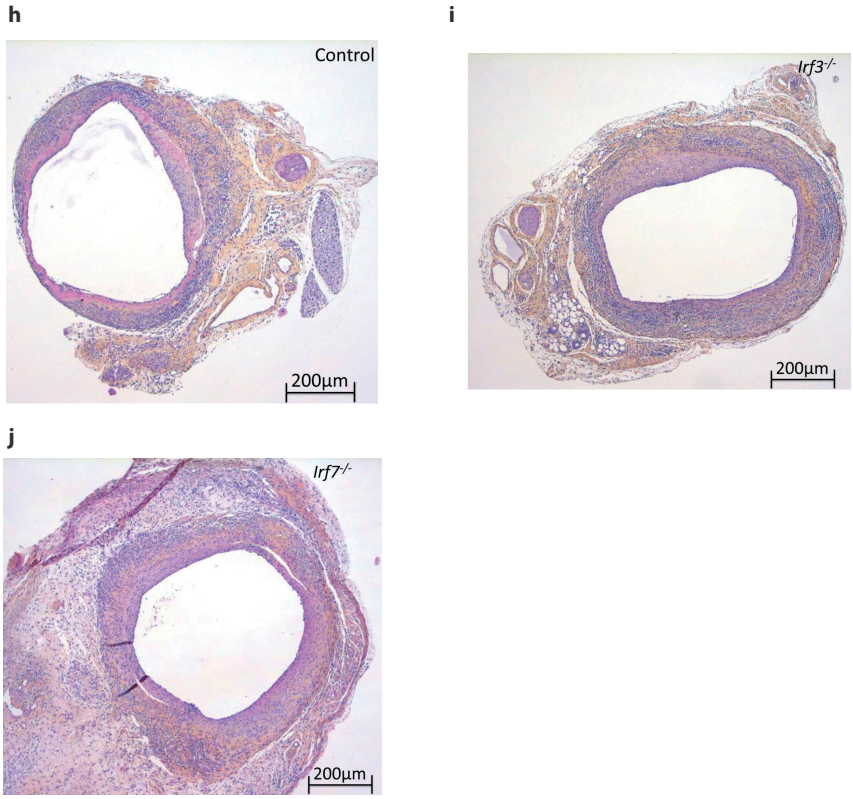

Figure 5. a. Representative picture of a vein graft of control mice stained with IRF3 and **b.** IRF7. 20x magnification. **c.** and **d.** Vessel wall area (mm^2) in caval veins at day of the surgery (t=0) and vein grafts 7, 14 and 28 days after sacrifice (t=7, t=14 and t=28 respectively) of *Irf3*$^{-/-}$, *Irf7*$^{-/-}$ and control mice. *p<0.05, **p<0.01, ***p<0.001. n=3-9 **e.** Representative picture of a control vein graft after 28 days, stained with Hematoxylin, Phloxine and Saffron **f.** vein graft of *Irf3*$^{-/-}$ mice **g.** and a vein graft of *Irf7*$^{-/-}$ mice. 5x magnification.

Intimal hyperplasia formation in IRF3 and IRF7 deficient mice is caused by macrophage accumulation.

To determine the percentage of inflammatory cells in the vein graft lesion, percentage of macrophages was determined. No differences were observed for the percentage macrophages in the vein grafts of *Irf3*$^{-/-}$ and *Irf7*$^{-/-}$ mice compared to control (table 1) sacrificed after 7 days. In vein grafts sacrificed after 14 days, *Irf3*$^{-/-}$ vein grafts showed a 89% increase of macrophages compared to control vein grafts (p=0.008) and no differences compared to *Irf7*$^{-/-}$ vein grafts (table 1). However, analysis of the vein grafts of mice sacrificed after 28 days, showed that the macrophage score was increased by 23% in *Irf7*$^{-/-}$ (p=0.04) vein grafts compared to control vein grafts and showed a trend towards an increase in *Irf3*$^{-/-}$ (p= 0.06) vein grafts compared to the control vein grafts (figure 6a). No differences between *Irf7*$^{-/-}$ and *Irf3*$^{-/-}$ vein grafts were observed after 28

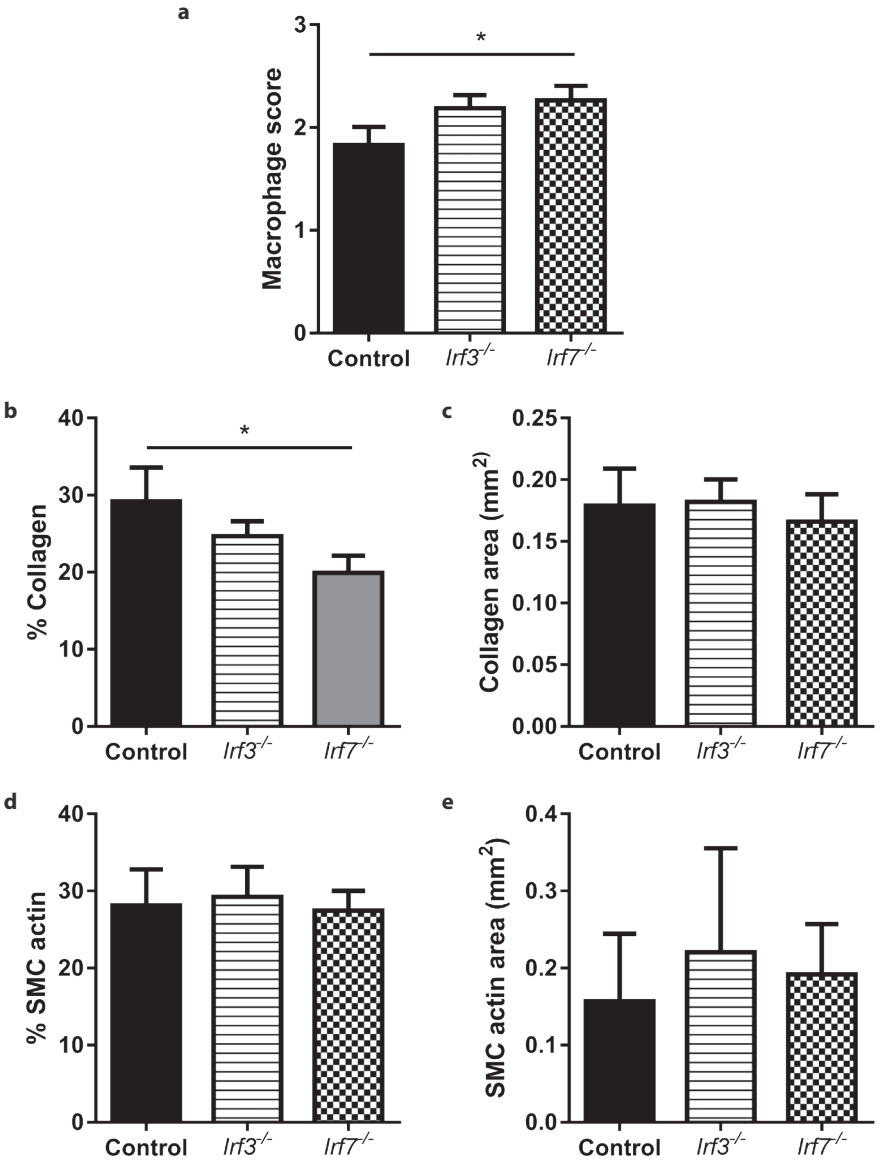

Figure 6 (Immuno)histological analysis of vein grafts of *Irf3*$^{-/-}$, *Irf7*$^{-/-}$ and control mice sacrificed after 28 days. **a.** Macrophage score **b.** Percentage of the collagen content and **c.** absolute numbers of the collagen content (mm^2). **d.** Percentage of the SMC actin content and **e.** absolute numbers of the smooth muscle cell content (mm^2). *p<0.05. n=8/group.

days. In conclusion, we here show an increased macrophage accumulation in the vein grafts of *Irf3*$^{-/-}$ mice after 14 days and vein grafts of *Irf7*$^{-/-}$ mice compared to control vein grafts 28 days after surgery.

	Irf3$^{-/-}$			**Irf7**$^{-/-}$		
	t=7	t=14	t=28	t=7	t=14	t=28
MAC-3	-8,13	89,68**	19,63	0,85	40,55	23,73*
aSMActin	-0,25	17,17	40,75	-9,51	39,75	22,38
Collagen	21,82	-74,38*	-15,47	1,11	-29,70	-19,33*

Table 1. In vein grafts of *Irf3*$^{-/-}$, *Irf7*$^{-/-}$ and control mice (immuno)histochemical stainings of, macrophages (MAC-3), smooth muscle cells (aSMActin) and collagen were performed to determine plaque composition. Stainings were performed on vein grafts harvested 7 days after surgery (t=7), 14 days (t=14) or 28 days after surgery (t=28). Percentages of changes compared to control vein grafts are shown. *p<0.05, **p<0.01

IRF7 deficiency induces smooth muscle cell proliferation.

To determine lesion stability, collagen content was determined. To determine the percentage of VSMCs and the percentage of proliferating VSMCs in *Irf7*$^{-/-}$ compared to *Irf3*$^{-/-}$ vein grafts, we performed a double immunohistochemical staining for proliferation marker Ki67 with vascular smooth muscle cell marker aSMActin.

No differences were observed in the percentage collagen in the vein grafts of *Irf3*$^{-/-}$ and *Irf7*$^{-/-}$ mice compared to control vein graft sacrificed after 7 days (table 1). The percentage of collagen in the vessel wall was significantly decreased in vein grafts of *Irf3*$^{-/-}$ mice compared to control vein grafts (p=0.001) and compared to *Irf7*$^{-/-}$ vein grafts (p=0.008) after 14 days and decreased in vein grafts of *Irf7*$^{-/-}$ mice (p=0.03) compared to control vein grafts after 28 days (figure 6b), indicating unstable lesions in *Irf3*$^{-/-}$ vein grafts after 14 days and in *Irf7*$^{-/-}$ vein grafts after 28 days. However, no differences were observed in the collagen area (mm^2) after 28 days (figure 6c).

The percentage of VSMCs (figure 6d) and the SMC area (mm^2) (figure 6e) was similar in both *Irf3*$^{-/-}$ and *Irf7*$^{-/-}$ mice compared to the control group after 28 days. In time, the percentage of SMCs increased in *Irf3*$^{-/-}$ vein grafts compared to control vein grafts.

We detected a higher percentage of proliferating VSMCs in *Irf7*$^{-/-}$ vein grafts compared to control vein grafts (figure 7a), with a trend toward an increase in *Irf3*$^{-/-}$ vein grafts compared to control vein grafts.

IRF3 and IRF7 differentially regulate type-I interferon (inducible) genes in vein grafts.

We previously showed a regulation of type-I IFN mRNA expression (figure 2) and IFNβ mRNA expression (figure 3) via IRF3 and IRF7 in vitro in VSMCs and BMM. To show that type-I IFN (inducible) genes are regulated by IRF3 and IRF7 in vivo in vein grafts, we performed a specific RT^2 profiler array with 84 type-I IFN response genes on pools of Irf3$^{-/-}$, Irf7$^{-/-}$ and control vein grafts (n=6 mice/group) sacrificed after 28 days. Up regulation of expression in the Irf3$^{-/-}$ and Irf7$^{-/-}$ mice was only found for a few genes (table 2a). Deficiency of IRF3 and IRF7 resulted in a decrease in specific type-I IFN inducible genes such as Ifit1, Ifit3 and Isg15. Irf3$^{-/-}$ vein grafts showed a down regulation of more than 2 fold in 16 specific type-I IFN inducible, were Irf7$^{-/-}$ vein graft showed a down regulation in 27 specific type-I IFN inducible genes (table 2b), which is 1.7 fold more compared to IRF3 vein grafts. In conclusion, we here show an IRF3 and IRF7 dependent regulation of type-I IFN (inducible) genes, with a more prominent role of IRF7 in the regulation of type-I IFN (inducible) genes.

Discussion

The present study is the first to describe a role for both IRF3 and IRF7 in vein graft disease and we here show that IRF3 and IRF7 regulate type-I IFNs via TLRs. IRF3 and IRF7 are highly expressed in vein grafts and IRF3 and IRF7 deficient mice show an increase in vein graft vessel wall thickening in comparison to control mice, indicating a protective role of both IRF3 and IRF7 in vein graft disease. Interestingly, deficiency of either IRF3 or IRF7 had a different effect on the vessel wall thickening in time. We here show an increased vessel wall thickening in vein grafts of *Irf3*$^{-/-}$ mice after 14 days, whereas vein grafts of *Irf7*$^{-/-}$ mice showed increased vessel wall thickening after 28 days. We also show a regulation of type-I IFNs via both IRF3 and IRF7 downstream of TLR3 activation and of pro-inflammatory cytokines only via IRF3 downstream TLR4 activation *in vitro*, in VSMCs and macrophages, prominent cell types in vein graft disease.

Previous studies showed a protective effect of IRF7 against VSMC proliferation and neointima formation in a mouse carotid artery wire injury model and carotid artery balloon injury model[24]. A protective effect of IRF3 on neointima formation was observed through inhibition of VSMC proliferation via PPARγ activation in a mouse carotid artery wire injury model[25]. All these findings are in line with our study, since we also showed a protective effect of both IRF3 and IRF7 in a vein graft model (figure 5c) and a decrease in VMSC proliferation in *Irf3*$^{-/-}$ mice compared to *Irf7*$^{-/-}$ mice (figure 7).

Gene Symbol	Irf3$^{-/-}$	Irf7$^{-/-}$
Crp	2,52	6,17
H2-Bl	3,6	3,79
H2-M10.1	3,39	2,62
Met	2,13	4,1
MGDC	<2	**2,02**
Ifne	<2	**5,36**
Ifna2	<2	**2,23**
Ifna4	**2,18**	<2
Myd88	<2	<2
Gbp1	<2	<2
Il10	<2	<2
Irf1	<2	<2
Irf2	<2	<2
Casp1	<2	<2
Nos2	<2	<2
Psme2	<2	<2
Stat1	<2	<2
Vegfa	<2	<2
Sh2d1a	**2,57**	<2
Ccl5	**3,89**	<2
Cav1	<2	**2,04**

a.

Gene Symbol	Irf3$^{-/-}$	Irf7$^{-/-}$	Gene Symbol	Irf3$^{-/-}$	Irf7$^{-/-}$
Ccl2	< -2	< -2	Ifitm2	**-2,01**	< -2
Cxcl10	< -2	**-9,07**	Mx1	-2,28	-20,99
Ifit1	-3,86	-9,97	Mx2	-2,87	-5,48
Ifit2	-3,73	-8,12	Nos2	**-2,12**	< -2
Ifit3	-5,31	-10,27	Oas2	-6,06	-11,47
Il6	**-6,34**	< -2	Stat1	< -2	**-2,59**
Isg15	-4,01	-8,08	Stat2	-2,1	-2,8
Oas1a	< -2	**-6,86**	Timp1	**-3,31**	< -2
Oas1b	< -2	**-4,08**	Ccl5	< -2	**-2,62**
Tlr7	< -2	< -2	Cd69	< -2	**-7,36**
Mal	< -2	**-2,04**	Cd70	< -2	**-4,44**
Bst2	< -2	**-2,04**	Eif2ak2	< -2	**-2,07**
Ifnz	< -2	< -2	Gbp1	< -2	**-2,29**
Irf7	-5,37	-159,22	H2-K1	< -2	**-2,67**
Sh2d1a	< -2	-4,63	H2-T10	< -2	**-2,96**
Tlr3	< -2	< -2	Ifih1	< -2	**-3,95**
Tlr7	< -2	< -2	Socs1	< -2	**-2,35**
Tlr9	< -2	**-3,15**	Tap1	< -2	**-2,74**
Ddx58	-2,01	-2,88			
Ifi204	**-2,04**	< -2			
Ifih1	**-3,15**	< -2			

b.

Table 2. RT^2 profiler array of type-I IFNs on pools of vein grafts of *Irf3*$^{-/-}$ and *Irf7*$^{-/-}$ mice are shown compared to control vein grafts. Data are expressed as fold induction. **a.** Genes that are up regulated more than 2-fold in one of the strains are shown in bold. **b.** Genes that are down regulated more than 2-fold are shown in bold.

IRF3 and IRF7 signaling pathways are extensively investigated in various processes and cell types. However signaling downstream TLRs is complex and can be different per cell type[26]. We here investigated VSMCs and macrophages. Based on our *in vitro* and *in vivo* experiments, we suggest the current model (figure 8) as downstream TLR3 and TLR4 signaling pathways, playing a role in vein graft disease. TLR3 signaling is known to be TRIF mediated, leading to type-I IFN activation[27], whereas TLR4 signaling is TRIF and Myd88 dependent, leading to pro-inflammatory cytokine activation and type-I IFN activation[4, 10]. However, we showed that TLR3 activation can also lead to pro-inflammatory cytokine production (figure 1). Previously it was shown that IRF3 is a downstream transcription factor that regulates the expression of IFNβ induced by

TRIF-dependent TLRs[28, 29]. However, NF-κB can also induce IFNβ gene expression in presence of IRF3 and it was shown that IRF3 can also be regulated downstream TLR4[27, 30-32], which is in line with our results (figure 1 and 2), since we also show an increased IFNβ gene expression regulated via IRF3 after TLR4 stimulation in BMM compared to unstimulated BMM . NF-κB was shown to induce interferon-stimulated genes independently of type-I IFN *in vivo*[33]. Besides, in response to LPS, it had been shown that IRF3 can be activated in a MyD88-independent manner[34, 35]. IFNβ gene induction in response to TLR4 ligation can be mediated by IRF3 in peritoneal macrophages and fibroblasts[28], but under certain conditions, IRF7 might also participate in TLR4 signaling, which was shown in dendritic cells[36], presumably also being activated by TBK1, an essential components of the IRF3 signaling pathway[31]. However, we showed that IRF7 is only involved in type-I IFN production and IRF3 in both type-I IFN and pro-inflammatory cytokine production in BMMs (figure 4).

Besides different signaling pathways downstream TLRs, IRF3 and IRF7 also showed to have different functions in time. Vessel wall thickening was increased in vein grafts of *Irf3*$^{-/-}$ mice after 14 days compared to vein grafts of *Irf7*$^{-/-}$ and control mice, whereas vein grafts of *Irf7*$^{-/-}$ mice showed a remarkable vessel wall thickening compared to vein grafts of *Irf3*$^{-/-}$ and control mice after 28 days. In line with this, in vein grafts of *Irf3*$^{-/-}$ mice, macrophage accumulation was seen after 14 days with a lower percentage of collagen in the vessel wall, whereas more macrophages and less collagen were seen in vein grafts of *Irf7*$^{-/-}$ mice after 28 days, indicating that a thickening of the vein graft vessel wall is unstable. Besides, after 28 days, the expression of type-I IFN was up regulated in *Irf7*$^{-/-}$ vein grafts compared to *Irf3*$^{-/-}$ vein grafts (table 2) and *Irf7*$^{-/-}$ vein grafts showed more proliferating VSMCs compared to *Irf3*$^{-/-}$ vein grafts. This different function of IRF3 and IRF7 in time can be explained by the fact that IRF3 is primarily responsible for the early induction phase of type-I IFNs and IRF7 is involved in the late induction phase of type-I IFNs as reported previously in responses to viral infections[17-19]. IRF3 is constitutively expressed and resides in the cytosol in a latent form and undergoes nuclear translocation following a stimulus such as a viral infection. IRF7 also resides in the cytosol and can be translocated to the nucleus following infection stimulus, but unlike IRF3, IRF7 is expressed in low amounts and is strongly induced by type-I IFNs via binding the type-I IFN receptor [4, 15]. IRF7 is in this way an inducer of a positive feedback loop of enhanced activation of type-I IFN [18, 19] which can result in stronger induction of type-I IFN (inducible) genes in the late phase, compared to IRF3 who act in the early phase with type-I IFN production[37]. In line with this, here we showed a more prominent role of IRF3 early in time and a late role for IRF7 *in vitro* (figure 4c) and *in vivo* (figure 5c). We here show a protective effect of IRF7 and IRF3 since vein grafts of *Irf3*$^{-/-}$ and *Irf7*$^{-/-}$ mice showed a reduction in vessel wall thickening compared to control vein grafts.

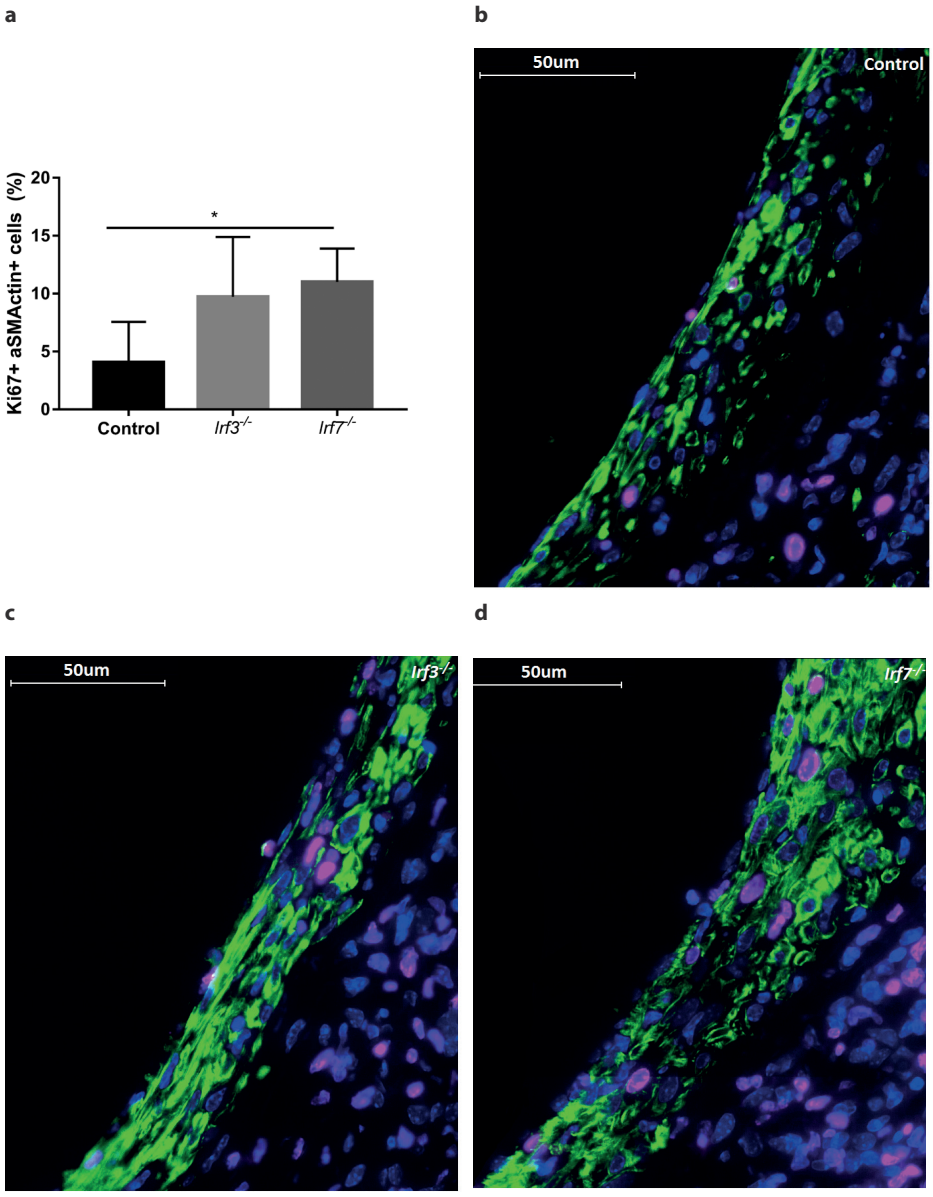

Figure 7. Vein grafts sacrificed after 28 days of *Irf3*$^{-/-}$, *Irf7*$^{-/-}$ and control mice were stained with proliferation marker Ki67 and with vascular smooth muscle cell marker aSMActin. **a.** percentage of dividing VSMCs (Ki67+ and aSMActin+) of total cells in shown. n=4, *p<0.05 **b.** Representative image of aSMActin (green) and Ki67 (magenta) immunofluorescence double staining in vein grafts are shown with DAPI (blue) of a control mice **c** *Irf3*$^{-/-}$ and **d.** *Irf7*$^{-/-}$ mice.

Furthermore, it has been shown that the contribution of IRF3 is minor in the absence of IRF7, probably due to the lack of IRF3 and IRF7 interaction[4]. So, to benefit from the protective effects of IRF3 and IRF7 in VGD, type-I IFN production must be increased in the early phase to induce IRF7 gene expression in the early phase, so IRF7 can contribute to the type-I IFN production along IRF3. However, in future experiments it must be taken in consideration that IRF3 and IRF7 can be present in an active or resting form, and their function can be cell specific. To investigate cell specific functions of IRF3 and IRF7, inducible knockouts can be used in the future, which will also exclude the genetically induced morphological differences in grafts used in our knockout mice.

We show an anti-inflammatory effect of type-I IFNs on vein graft vessel wall thickening, however, the mechanism behind this anti-inflammatory effect of type-I IFNs is complex. At first, the IFN system was shown to be part of the host innate immunity, through its antiviral functions, although activation of type-I IFN mediates a variety of immunoregulatory effect, suggesting an important link between innate and adaptive immunity[38]. Previous studies showed that *in vitro*, IFNβ inhibited human VSMC growth and VSMCs expressed the IFNβ gene and could thereby inhibit neointima formation[39]. *In vivo*, it was shown that an adenoviral vector encoding IFNβ reduced VSMC proliferation and intima hyperplasia in a porcine balloon injury model[40]. In line with these studies we showed an increased VSMC proliferation in *Irf7*$^{-/-}$ vein grafts compared to *Irf3*$^{-/-}$ vein grafts. Besides, it is shown that IFNβ has some anti-inflammatory roles in certain diseases[41], such as familiar Mediterranean fever [42], Behcet's syndrome[43] and relapsing-remitting MS[44]. A recent study described two potential anti-inflammatory mechanisms of type-I IFNs[22], via the inhibition of NLRP1 and NLRP3 inflammasome, or via induction of IL-10 who then through activation of STAT3 transcription factor reduced the abundance of pro-IL-1a and pro-IL-1β. Indicating that IFNβ can induce IL-10 and inhibit the inflammasome and thereby regulate vein graft disease, which is in line with previous studies who described an important role of the inflammasome in the pathophysiology of vein graft remodeling[45]. However, the exact mechanism of the protective effect of type-I IFNs in vein graft disease is still unknown and needs to be further investigated for optimal therapeutic application.

In conclusion, our study revealed a role for IRF3 and IRF7 in the regulation of vein graft vessel wall thickening via type-I IFNs. So far a protective role for IRF3 and IRF7 on vein graft vessel wall thickening is observed, giving rise to potential new strategies to use IRF3, IRF7 or type-I FNs in a therapeutic approach.

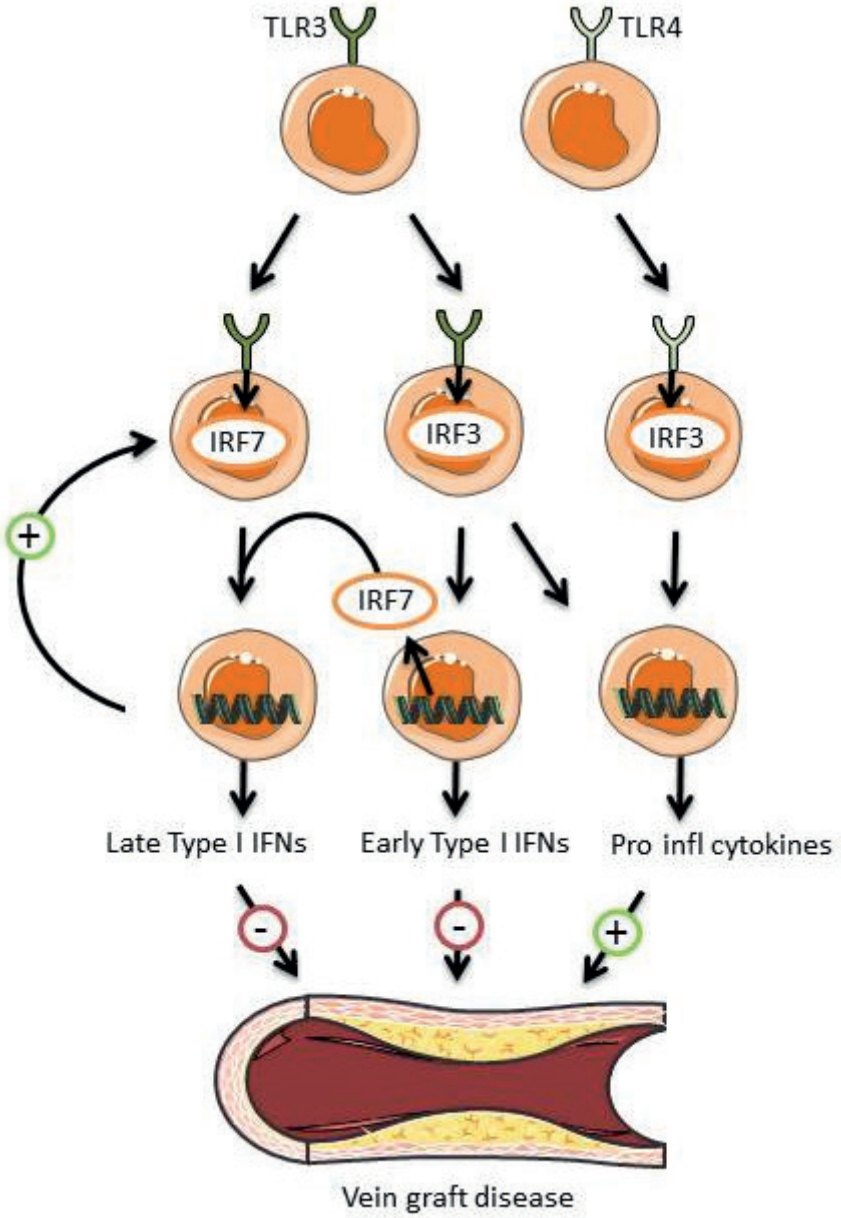

Figure 8. Model of signaling pathways through TLR3 and TLR4. Summary of *in vitro* and *in vivo* results.

References

1. de Vries M.R. Simons, K.H. Jukema, J.W. Braun, J. Quax, P.H.A. Vein graft failure: from pathophysiology to clinical outcomes. Nature Reviews Cardiology 2016;13(8):451–70.
2. Goldman S. Zadina, K. Moritz, T. Ovitt, T. Sethi, G. Copeland, J.G. Thottapurathu, L. Krasnicka, B. Ellis, N. Anderson, R.J. Henderson, W; VA Cooperative Study Group. Long-term patency of saphenous vein and left internal mammary artery grafts after coronary artery bypass surgery: results from a Department of Veterans Affairs Cooperative Study. J Am Coll Cardiol. 2004;44(11):2149–56.
3. Karper J.C. de Vries, M.R. van den Brand, B.T. Hoefer, I.E. Fischer, J.W. Jukema, J.W. Niessen, H.W. Quax, P.H.A. Toll-like receptor 4 is involved in human and mouse vein graft remodeling, and local gene silencing reduces vein graft disease in hypercholesterolemic APOE*3Leiden mice. Arterioscler Thromb Vasc Biol. 2011;5:1033-40.
4. Honda K. Taniguchi, T. IRFs: master regulators of signalling by Toll-like receptors and cytosolic pattern-recognition receptors. Nat Rev Immunol. 2006 6(9):644-58.
5. Karper J.C. Ewing, M.M. Habets, K.L. de Vries, M.R. Peters, H.A.B. van Oeveren-Rietdijk, A.M. de Boer, H.C. Hamming, J.F. Kuiper, J. Kandimalla, E.R. La Monica, N. Jukema, J.W. Quax, P.H.A. Blocking toll-like receptors 7 and 9 reduces postinterventional remodeling via reduced macrophage activation, foam cell formation, and migration. Arterioscler Thromb Vasc Biol. 2012;32(8):e72-80. Epub 2012/05/26. doi: 10.1161/atvbaha.112.249391. PubMed PMID: 22628437.
6. Sharma S. Garg, I. Ashraf, M.Z. TLR signalling and association of TLR polymorphism with cardiovascular diseases. Vascul Pharmacol 2016;87:30-7.
7. Cole J.E. Navin, T.J. Cross, A.J. Goddard, M.E. Alexopoulou, L. Mitra, A.T. Davies, A.H. Flavell, R.A. Feldmann, M. Monaco, C. Unexpected protective role for Toll-like receptor 3 in the arterial wall. Proc Natl Acad Sci U S A 2010;108(6):2372–7.
8. Zimmer S. Steinmetz, M. Asdonk, T. Motz, I. Coch, C. Hartmann, E. Barchet, W. Wassmann, S. Hartmann, G. Nickenig, G. Activation of endothelial toll-like receptor 3 impairs endothelial function. Circ Res 2011;108(11):1358-66.
9. Richards M.R. Black, A.S. Bonnet, D.J. Barish, G.D. Woo, C.W. Tabas, I. Curtiss, L.K. Tobias, P.S. The LPS2 mutation in TRIF is atheroprotective in hyperlipidemic low density lipoprotein receptor knockout mice. Innate immun. 2013;19(1):20-9.
10. Kawai T. Akira, S. The role of pattern-recognition receptors in innate immunity: update on Toll-like receptors. Nat Immunol. 2010;11(5):373-84.
11. González-Navajas J.M. Lee, J. David, M. Raz, E. Immunomodulatory functions of type I interferons. Nat Rev Immunol 2012;12(2):125-35.
12. Teunissen P. F. Boshuizen, M. C. Hollander, M. R. Biesbroek, P. S. van der Hoeven, N. W. Mol, J. Q. Gijbels, M. J. van der Velden, S. van der Pouw Kraan, T. C. Horrevoets, A. J. de Winther, M. P. van Royen, N. MAb therapy against the IFN-alpha/beta receptor subunit 1 stimulates arteriogenesis in a murine hindlimb ischaemia model without enhancing atherosclerotic burden. Cardiovasc Res. 2015;107(2):255-66. Epub 2015/05/04. doi: 10.1093/cvr/cvv138. PubMed PMID: 25935869.
13. Barnes B. Lubyova, B. Pitha, P.M. Review: On the Role of IRF in Host Defense. Journal of Interferon & Cytokine Research. 2004;22(1):59-71.
14. Juang Y.T. Lowther, W. Kellum, M. Au, W.C. Lin, R. Hiscott, J. Pitha, P.M. . Primary activation of interferon A and interferon B gene transcription by interferon regulatory factor 3. Proc Natl Acad Sci USA. 1998;95(17):9837–42.
15. Ning S. Pagano, J.S. Barber, G.N. IRF7: activation, regulation, modification and function. Genes Immun. 2011;12(6):399-414. Epub 2011/04/15. doi: 10.1038/gene.2011.21. PubMed PMID: 21490621; PubMed Central PMCID: PMCPMC4437765.

16. Decker T. Muller, M. Stockinger, S. The yin and yang of type I interferon activity in bacterial infection. Nat Rev Immunol. 2005;5(9):675-87. Epub 2005/08/20. doi: 10.1038/nri1684. PubMed PMID: 16110316.
17. Sato M. Suemori, H. Hata, N. Asagiri, M. Ogasawara, K. Nakao, K. Nakaya, T. Katsuki, M. Noguchi, S. Tanaka, N. Taniguchi, T. Distinct and essential roles of transcription factors IRF-3 and IRF-7 in response to viruses for IFN-alpha/beta gene induction. Immunity. 2000;13(4):539-48.
18. Sato M. Hata, N. Asagiri, M. Nakaya, T. Taniguchi, T. Tanaka, N. Positive feedback regulation of type I IFN genes by the IFN-inducible transcription factor IRF-7. FEBS lett. 1998;441(1):106-10.
19. Marié I. Durbin, J.E. Levy, D.E. Differential viral induction of distinct interferon-alpha genes by positive feedback through interferon regulatory factor-7. EMBO J. 1998;17(22):6660-9.
20. Jiang D.S. Liu, Y. Zhou, H. Zhang, Y. Zhang, X.D. Zhang, X.F. Chen, K. Gao, L. Peng, J. Gong, H. Chen, Y. Yang, Q, Liu, P.P. Fan, G.C. Zou, Y. Li, H. Interferon regulatory factor 7 functions as a novel negative regulator of pathological cardiac hypertrophy. Hypertension. 2014;63(4):713-22.
21. Wang X. Chen, M. Wandinger, K.P. Williams, G. Dhib-Jalbut, S. IFN-β-1b inhibits IL-12 production in peripheral blood mononuclear cells in an IL-10-dependent mechanism: relevance to IFN-β-1b therapeutic effects in multiple sclerosis. J Immunol. 2000;165:548–57.
22. Guarda G. Braun, M. Staehli, F. Tardivel, A. Mattmann, C. Förster, I. Farlik, M. Decker, T. Du Pasquier, R.A. Romero, P. Tschopp, J. Type I interferon inhibits interleukin-1 production and inflammasome activation. Immunity. 2011 34(2):213-23.
23. de Vries M.R. Wezel, A. Schepers, A. van Santbrink, P.J. Woodruff, T.M. Niessen, H.W. Hamming, J.F. Kuiper, J. Bot, I. Quax, P.H.A. Complement Factor C5a as Mast cell Activator mediates Vascular Remodeling in Vein Graft Disease. Cardiovasc Res. 2013;97(2):311-20.
24. Huang L. Zhang, S.M. Zhang, P. Zhang, X.J. Zhu, L.H. Chen, K. Gao, L. Zhang, Y. Kong, X.J. Tian, S. Zhang, X.D. Li, H. Interferon regulatory factor 7 protects against vascular smooth muscle cell proliferation and neointima formation. J Am Heart Assoc. 2014;3(5):e001309.
25. Zhang S.M. Zhu, L.H. Li, Z.Z. Wang, P.X. Chen, H.Z. Guan, H.J. Jiang, D.S. Chen, K. Zhang, X.F. Tian, S. Yang, D. Zhang, X.D. Li, H. Interferon regulatory factor 3 protects against adverse neo-intima formation. Cardiovasc Res. 2014 102(3):469-79.
26. Karper J. C. de Jager, S. C. Ewing, M. M. de Vries, M. R. Bot, I. van Santbrink, P. J. Redeker, A. Mallat, Z. Binder, C. J. Arens, R. Jukema, J. W. Kuiper, J. Quax, P. H. An unexpected intriguing effect of Toll-like receptor regulator RP105 (CD180) on atherosclerosis formation with alterations on B-cell activation. Arterioscler Thromb Vasc Biol. 2013;33(12):2810-7. Epub 2013/10/12. doi: 10.1161/atvbaha.113.301882. PubMed PMID: 24115036.
27. Akira S. Takeda, K. Toll-like receptor signalling. Nat Rev Immunol. 2004;4(7):499-511.
28. Kawai T Takeuchi O, Fujita T, Inoue J, Mühlradt PF, Sato S, Hoshino K, Akira S. Lipopolysaccharide stimulates the MyD88-independent pathway and results in activation of IFN-regulatory factor 3 and the expression of a subset of lipopolysaccharide-inducible genes. J Immunol 2001;167(10):5887-94.
29. Yamamoto M. Yamazaki, S. Uematsu, S. Sato, S. Hemmi, H. Hoshino, K. Kaisho, T. Kuwata, H. Takeuchi, O. Takeshige, K. Saitoh, T. Yamaoka, S. Yamamoto, N. Yamamoto, S. Muta, T. Takeda, K. Akira, S. Regulation of Toll/IL-1-receptor-mediated gene expression by the inducible nuclear protein IκBζ. Nature. 2004;430:218-22.
30. Ho C.C. Luo, Y.H. Chuang, T.H. Lin, P. Quantum dots induced interferon beta expression via TRIF-dependent signaling pathways by promoting endocytosis of TLR4. Toxicology. 2016;344-366:61-70.
31. Fitzgerald K.A. McWhirter, S.M. Faia, K.L. Rowe, D.C. Latz, E. Golenbock, D.T. Coyle, A.J. Liao, S.M. Maniatis, T. IKKepsilon and TBK1 are essential components of the IRF3 signaling pathway. Nature Immunology. 2003;4:491-6.
32. Doyle S. Vaidya, S. O'Connell, R. Dadgostar, H. Dempsey, P. Wu, T. Rao, G. Sun, R. Haberland, M. Modlin, R. Cheng, G. IRF3 Mediates a TLR3/TLR4-Specific Antiviral Gene Program. Immunity. 2002;17(3):251-63.

33. Rubio D. Xu, R.H. Remakus, S. Krouse, T.E. Truckenmiller, M.E. Thapa, R.J. Balachandran, S. Alcamí, A. Norbury, C.C. Sigal, L.J. Crosstalk between the Type 1 Interferon and Nuclear Factor Kappa B Pathways Confers Resistance to a Lethal Virus Infection. Cell host & Microbe. 2013;13(6):701-10.
34. Nakaya T. Sato, M. Hata, N. Asagiri, M. Suemori, H. Noguchi, S. Tanaka, N. Taniguchi, T. Gene induction pathways mediated by distinct IRFs during viral infection. Biochem Biophys Res Commun. 2001;283(5):1150-6.
35. Toshchakov V. Jones, B.W. Perera, P.Y. Thomas, K. Cody, M.J. Zhang, S. Williams, B.R. Major, J. Hamilton, T.A. Fenton, M.J. Vogel, S.N. TLR4, but not TLR2, mediates IFN-beta-induced STAT1alpha/beta-dependent gene expression in macrophages. Nature Immunology. 2002;3(4):392-8. Epub 2002 Mar 18.
36. Sakaguchi S. Negishi, H. Asagiri, M. Nakajima, C. Mizutani, T. Takaoka, A. Honda, K. Taniguchi, T. Essential role of IRF-3 in lipopolysaccharide-induced interferon-beta gene expression and endotoxin shock. Biochem Biophys Res Commun. 2003;306(4):860-6.
37. Lin R. Mamane, Y. Hiscott, J. Multiple regulatory domains control IRF-7 activity in response to virus infection. J Biol Chem. 2000 275(44):34320-7.
38. CA Biron. Interferons alpha and beta as immune regulators; a new look. Immunity. 2001;14(6):661-4.
39. Palmer H Libby P. Interferon-beta. A potential autocrine regulator of human vascular smooth muscle cell growth. Lab Invest. 1992 66(6):715-21.
40. Stephan D. San, H. Yang, Z.Y. Gordon, D. Goelz, S. Nabel, G.J. Nabel, E.G. Inhibition of vascular smooth muscle cell proliferation and intimal hyperplasia by gene transfer of beta-interferon. Mol Med. 1997;3(9):593-9.
41. Choubey D. Moudgil, K.D. Interferons in Autoimmune and Inflammatory Diseases: Regulation and Roles. Journal of interferon and cytokine research. 2011;31(12):857-65.
42. Tweezer-Zaks N. Rabinovich, E. Lidar, M. Livneh, A. Interferon-alpha as a treatment modality for colchicine-resistant familial Mediterranean fever. J Rheumatol. 2008;35(7):1362-5.
43. Kötter I. Zierhut, M. Eckstein, A.K. Vonthein, R. Ness, T. Günaydin, I. Grimbacher, B. Blaschke, S. Meyer-Riemann, W. Peter, H.H. Stübiger, N. Human recombinant interferon alfa-2a for the treatment of Behçet's disease with sight threatening posterior or panuveitis. Br J Ophthalmol. 2003;87(4):423-31.
44. Billiau A. Anti-inflammatory properties of Type I interferons. Antiviral Res. 2006;71(2-3):108-16.
45. Li P. Li, Y.L. Li, Z.Y. Wu,Y.N. Zhang, C.C. A, X. Wang, C.X. Shi, H.T. Hui, M.Z. Xie, B. Ahmed, M. Du, J. Cross Talk Between Vascular Smooth Muscle Cellsn and Monocytes Through Interleukin-1β/Interleukin-18 Signaling Promotes Vein Graft Thickening. Arterioscler Thromb Vasc Biol. 2014.;34:2001-11.

Supplemental figures

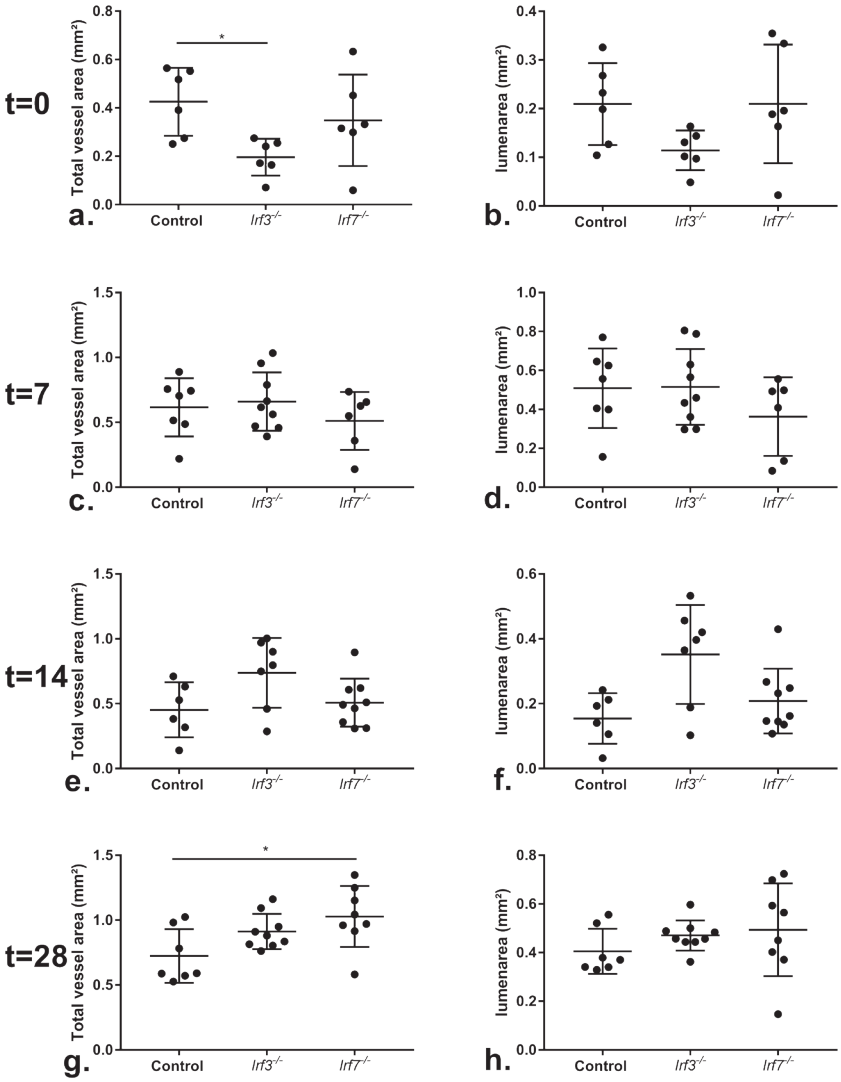

Figure S1. Total vessel wall area (**a,c,e,g**) and lumen area (**b,d,f,h**) of *Irf3*$^{-/-}$, *Irf7*$^{-/-}$ and control mice, sacrificed after 0, 7, 14 and 28 days. *p<0.05, n=6-9.